Available online at www.sciencedirect.com
SCIENCE DIRECT®
International Journal of Heat and Fluid Flow 26 (2005) 732–745
International Journal of HEAT AND FLUID FLOW
www.elsevier.com/locate/ijhff

An explicit algebraic Reynolds stress model based on a nonlinear pressure strain rate model

Olof Grundestam [a,*], Stefan Wallin [a,b], Arne V. Johansson [a]

[a] Department of Mechanics, Royal Institute of Technology, KTH, SE-100 44 Stockholm, Sweden
[b] Aeronautics Division, FFA, Swedish Defence Research Agency (FOI), SE-172 90 Stockholm, Sweden

Received 6 May 2004; received in revised form 19 April 2005; accepted 28 April 2005
Available online 11 July 2005

Abstract

The use of a pressure strain rate model including terms nonlinear in the mean strain and rotation rate tensors in an explicit algebraic Reynolds stress model (EARSM) is considered. For 2D mean flows the nonlinear contributions can be fully accounted for in the EARSM formulation. This is not the case for 3D mean flows and a suggestion of how to modify the nonlinear terms to make the EARSM formulation in 3D mean flows consistent with its 2D counterpart is given. The corresponding EARSM is derived in conjunction with the use of streamline curvature corrections emanating from the advection of the Reynolds stress anisotropy. The proposed model is tested for rotating homogeneous shear flow, rotating channel flow and rotating pipe flow and the nonlinear contributions are shown to have a significant effect on the predicted flow characteristics. In cases where the 3D effects are strong, the approximations of the production to dissipation ratio made in the EARSM formulation for 3D mean flows must be made carefully and a 3D mean flow correction is considered. For the rotating pipe flow at the highest rotation rate investigated, the standard formulation even prevented convergence, while inclusion of the 3D correction gives reasonable results.

Keywords: Turbulence modelling; EARSM; Nonlinear modelling; Rotating flow; Projection method

1. Introduction

The endeavour to construct engineering turbulence models with a high degree of generality is a challenge of significant importance for the improvement of the predictive capability of CFD codes. In particular, effects of strong curvature and rotation represent cornerstone problems in turbulence modelling. The widely used traditional two equation models with the Boussinesq hypothesis are particularly ill suited for these types of flows since this family of model equations are insensitive to rotation in the standard formulation.

The effects of system rotation and/or mean streamline curvature on the turbulence are of complex nature. One of the primary effects is the influence on inter-component energy transfer, which in turn affects the turbulence production and can give damping as well as enhancement of the turbulence. In the transport equations for the Reynolds stress tensor in a rotating system the Coriolis force gives rise to redistribution terms, which play a major role in this context. In differential Reynolds stress models (DRSM) these terms enter explicitly, while the redistribution associated with the pressure–strain correlation forms a key issue in the modelling at this level.

The limitations of DRSM to capture the more subtle effects of rotation were illustrated by e.g. Leuchter and Cambon (1996) for the case of axisymmetric turbulence subjected to a combined axial strain and rotation. Generalizations of the DRSM concept have been studied by

* Corresponding author.
E-mail addresses: olof@mech.kth.se (O. Grundestam), stefan.wallin@foi.se (S. Wallin), viktor@mech.kth.se (A.V. Johansson).

0142-727X/$ - see front matter © 2005 Elsevier Inc. All rights reserved.
doi:10.1016/j.ijheatfluidflow.2005.04.004

several authors but are typically more useful for the study of turbulence dynamics and general properties of modelling than for engineering type of computations in complex geometries. An interesting example is the structure based model of Kassinos et al. (2001), see also Poroseva et al. (2002). A somewhat similar approach was studied by Johansson (1995).

A DRSM approach with models nonlinear in the anisotropy was proposed by Sjögren and Johansson (2000). The models for the individual terms were constructed to ensure realizability at the two-component limit (e.g. at solid walls). An obvious advantage that this approach offers is a reduction of the need for ad hoc wall-damping functions (see also Johansson and Hallbäck, 1994). Extensions including terms nonlinear in the mean velocity gradients were also proposed. These were shown to extend the capability of the DRSM to capture more subtle effects of rotation, such as the damped oscillations of the anisotropy observed in homogeneous turbulence subject to rotation (Mansour et al., 1991). This behaviour cannot be captured by a DRSM using a pressure strain rate model that is linear in the mean velocity gradients.

Explicit algebraic Reynolds stress models (EARSM) have attracted much attention during the last decade and have the advantage that the well established and well tested codes based on eddy-viscosity two-equation models can be used with a moderate amount of modification. The Boussinesq hypothesis is here replaced by a relation for the Reynolds stress anisotropy that is obtained from an algebraic approximation of the Reynolds stress transport equations. In the standard formulation of an EARSM the advection and diffusion terms in the transport equation for the Reynolds stress anisotropy are neglected in an inertial frame of reference. The underlying models for the individual terms (e.g. pressure strain rate) have been linear or quasi-linear in order to obtain solvable systems of equations that give the resulting EARSM. Several authors (e.g. Girimaji, 1997, Gatski and Jongen, 2000 and Wallin and Johansson, 2002) have also proposed EARSM formulations where corrections for mean streamline curvature are included in the algebraic representation. This can improve the predictive capability of an EARSM in flows where the effect of curvature and rotation are strong.

Here, we explore the possibility of constructing EARSMs based on pressure strain rate models that include terms nonlinear in the mean velocity gradients. These terms were first introduced by Sjögren and Johansson (2000) and were demonstrated to improve predictions in rotating flows. Since the new contributions are only nonlinear in the mean velocity gradients they can be expected to be relatively easy to include in an EARSM since they do not introduce any nonlinearities of the Reynolds stress anisotropy in the implicit relation. Terms tensorially nonlinear in Reynolds stress anisotropy are also discussed. They are, however, not included in the proposed model.

An EARSM is derived from the transport equation for the Reynolds stress anisotropy which in a nonrotating inertial frame of reference reads

$$K\frac{\mathrm{D}a_{ij}}{\mathrm{D}t}-\underbrace{\left(\frac{\partial T_{ijl}}{\partial x_l}-\frac{\overline{u_iu_j}}{K}\frac{\partial T_l^{(K)}}{\partial x_l}\right)}_{KD_{ij}^{(a)}}=-\frac{\overline{u_iu_j}}{K}(\mathscr{P}-\varepsilon)+\mathscr{P}_{ij}-\varepsilon_{ij}+\Pi_{ij} \tag{1}$$

in cartesian tensor notation. $\mathrm{D}/\mathrm{D}t$ is the advective derivative defined as $\mathrm{D}/\mathrm{D}t=\partial/\partial t+U_j\partial/\partial x_j$ in cartesian coordinates. $T_{ijl}=\overline{u_iu_ju_l}+(\overline{pu_i}\delta_{jl}+\overline{pu_j}\delta_{il})/\rho$ represents the total diffusion of the Reynolds stress components. $T_l^{(K)}$ is the diffusion of the turbulence kinetic energy and is given by $T_l^{(K)}=T_{iil}/2$. The dissipation rate tensor, ε_{ij}, and the pressure strain rate tensor, Π_{ij}, need to be modelled while the Reynolds stress production $\mathscr{P}_{ij}$ and the turbulence kinetic energy production $\mathscr{P}$ can be expressed explicitly in a_{ij}, K and the mean strain and rotation rate tensors. When normalized with the turbulence time scale ($\tau=K/\varepsilon$) the latter two read

$$S_{ij}\equiv\frac{\tau}{2}\left(\frac{\partial U_i}{\partial x_j}+\frac{\partial U_j}{\partial x_i}\right),\quad \Omega'_{ij}\equiv\frac{\tau}{2}\left(\frac{\partial U_i}{\partial x_j}-\frac{\partial U_j}{\partial x_i}\right) \tag{2}$$

If the flow is subject to rotation, one can, for convenience, express (1) in coordinates relative to the rotating frame. The transformation to this system gives rise to an additional contribution from the material derivative. This is of the form

$$C_{ij}=a_{ik}\Omega_{kj}^{(s)}-\Omega_{ik}^{(s)}a_{kj} \tag{3}$$

and is usually referred to as the Coriolis term and should be added to the right hand side of (1). The system rotation rate tensor, $\Omega_{ij}^{(s)}$, is defined as $\Omega_{ij}^{(s)}=-\tau\epsilon_{ijk}\omega_k^{(s)}$ and $\omega_k^{(s)}$ denotes the kth component of the constant rotation rate vector of the system. One must further account for the fact that the mean velocity (and therefore also the mean velocity gradient $\partial U_i/\partial x_j$) is not objective which means that the rotation rate tensor, due to the fact that it is antisymmetric, must be replaced by the absolute rotation rate tensor, Ω_{ij}, given by

$$\Omega_{ij}=\Omega'_{ij}+\Omega_{ij}^{(s)} \tag{4}$$

where Ω'_{ij} is expressed in coordinates relative to the rotating system. By applying (4) to the production term, an additional term identical to C_{ij} in (3) will appear on the right hand side of (1). This is the origin of the factor two in the Coriolis term in many publications. The strain rate tensor, on the other hand, preserves its form since it is symmetric. For a more thorough discussion on this, see Gatski and Wallin (2004).

An EARSM is based on the weak equilibrium assumption, Rodi (1976), which amounts to neglecting

the advection and diffusion of a_{ij}, i.e. the left hand side of (1). This yields a purely algebraic relation

$$\left(\mathbf{a}+\frac{2}{3}\mathbf{I}\right)\left(\frac{\mathscr{P}}{\varepsilon}-1\right)=\frac{1}{\varepsilon}(\mathscr{P}-\boldsymbol{\varepsilon}+\boldsymbol{\Pi}) \tag{5}$$

in boldface matrix notation in which $\mathscr{P}/\varepsilon \equiv -\{\mathbf{aS}\}$, where $\{\}$ denotes the trace and $\mathbf{I}$ is the identity matrix. The production of the Reynolds stresses normalized with the dissipation rate, can be expressed as

$$\frac{\mathscr{P}}{\varepsilon}=-\frac{4}{3}\mathbf{S}-(\mathbf{aS}+\mathbf{Sa})+\mathbf{a\Omega}-\mathbf{\Omega a} \tag{6}$$

The pressure strain rate and dissipation rate anisotropy ($e_{ij}=\varepsilon_{ij}/\varepsilon-2\delta_{ij}/3$) tensors can be lumped together and modelled, with the nonlinear contributions in addition to the general quasi-linear model, as

$$\frac{\boldsymbol{\Pi}}{\varepsilon}-\mathbf{e}=-\frac{1}{2}\left(C_1^0+C_1^1\frac{\mathscr{P}}{\varepsilon}\right)\mathbf{a}+C_2\mathbf{S}+\frac{C_3}{2}(\mathbf{aS}+\mathbf{Sa}-\frac{2}{3}\{\mathbf{aS}\}\mathbf{I})-\frac{C_4}{2}(\mathbf{a\Omega}-\mathbf{\Omega a})+C_\Omega(\mathbf{N}^\Omega+\mathbf{N}^S) \tag{7}$$

where the nonlinear terms are

$$\mathbf{N}^\Omega=\frac{1}{\sqrt{-II_\Omega}}\left(\mathbf{a\Omega}^2+\mathbf{\Omega}^2\mathbf{a}-\frac{2}{3}\{\mathbf{a\Omega}^2\}\mathbf{I}\right) \tag{8}$$

$$\mathbf{N}^S=\frac{1}{\sqrt{II_S}}\left(\mathbf{aS}^2+\mathbf{S}^2\mathbf{a}-\frac{2}{3}\{\mathbf{aS}^2\}\mathbf{I}\right). \tag{9}$$

$II_\Omega=\Omega_{ij}\Omega_{ji}$ and $II_S=S_{ij}S_{ji}$ are the second invariants of the rotation and strain rate tensors, respectively. $\mathbf{N}^\Omega$ and $\mathbf{N}^S$ were introduced by Sjögren and Johansson (2000) and were shown to improve the prediction of effects of rotation. By using the same model coefficient, C_Ω, for both $\mathbf{N}^\Omega$ and $\mathbf{N}^S$ their total contribution vanishes in parallel flows where $II_S=-II_\Omega$ e.g. channel flow and homogeneous shear flow.

The modelled transport equation of the Reynolds stress anisotropy can now be written

$$\tau\left(\frac{\mathrm{D}\mathbf{a}}{\mathrm{D}t}-\mathscr{D}^{(a)}\right)=A_0\left(\left(A_3+A_4\frac{\mathscr{P}}{\varepsilon}\right)\mathbf{a}+A_1\mathbf{S}-(\mathbf{a\Omega}-\mathbf{\Omega a})+A_2\left(\mathbf{aS}+\mathbf{Sa}-\frac{2}{3}\{\mathbf{aS}\}\mathbf{I}\right)-c(\mathbf{N}^\Omega+\mathbf{N}^S)\right) \tag{10}$$

The relations between the A and C-coefficients are

$$A_0=\frac{C_4}{2}-1,\quad A_1=\frac{3C_2-4}{3A_0}$$
$$A_2=\frac{C_3-2}{2A_0},\quad A_3=\frac{2-C_1^0}{2A_0} \tag{11}$$
$$A_4=\frac{-C_1^1-2}{2A_0},\quad c=-\frac{C_\Omega}{A_0}$$

After assuming weak equilibrium and hence neglecting the advection and diffusion (10) can, in analogy with (5), be written as an algebraic relation

$$N\mathbf{a}=-A_1\mathbf{S}+(\mathbf{a\Omega}-\mathbf{\Omega a})-A_2\left(\mathbf{aS}+\mathbf{Sa}-\frac{2}{3}\{\mathbf{aS}\}\mathbf{I}\right)+c(\mathbf{N}^\Omega+\mathbf{N}^S) \tag{12}$$

where $N=A_3+A_4\frac{\mathscr{P}}{\varepsilon}$.

2. Nonlinear modelling in conjunction with streamline curvature corrections

By imposing the weak equilibrium assumption in a curvilinear coordinate system that follows the mean flow, the advection gives rise to an additional algebraic term, see Girimaji (1997) and Sjögren (1997) that can be formulated as

$$\frac{\mathrm{D}\mathbf{a}}{\mathrm{D}t}\rightarrow-(\mathbf{a\Omega}^{(r)}-\mathbf{\Omega}^{(r)}\mathbf{a}) \tag{13}$$

The antisymmetric tensor $\mathbf{\Omega}^{(r)}$ is a measure of the local rotation rate following a mean flow streamline. Generally speaking, (13) will provide a systematic approximation of the advection if $\mathbf{\Omega}^{(r)}$ can be derived in the mean flow considered, see Girimaji (1997), Gatski and Jongen (2000) and Wallin and Johansson (2002). In the generic cases studied here, the curvature correction, (13), will fully account for the system rotation and hence include the contribution (3).

The application of the curvature correction leads to an EARSM formulation that depends on $\mathbf{S}$, $\mathbf{\Omega}$ and $\mathbf{\Omega}^{(r)}$, i.e. $a_{ij}=f_{ij}(\mathbf{S},\mathbf{\Omega},\mathbf{\Omega}^{(r)})$, rather than $\mathbf{S}$ and $\mathbf{\Omega}$ which is the case without the curvature correction, see Gatski and Wallin (2004). However, for a pressure strain rate model that is linear in $\mathbf{\Omega}$, this implies that the curvature correction can be included simply by transforming the absolute rotation rate tensor, $\mathbf{\Omega}$, as

$$\mathbf{\Omega}\rightarrow\mathbf{\Omega}^*=\mathbf{\Omega}-\frac{\tau}{A_0}\mathbf{\Omega}^{(r)} \tag{14}$$

This gives an EARSM formulation dependent on two tensors, $\mathbf{S}$ and $\mathbf{\Omega}^*$, according to $a_{ij}=g_{ij}(\mathbf{S},\mathbf{\Omega}^*)$.

When a pressure strain rate model that is nonlinear in $\mathbf{\Omega}$ is used, the inclusion of $\mathbf{N}^\Omega$ in our case, the transformation (14) is not valid, and the EARSM must be formulated in terms of the three tensors mentioned. For 2D mean flows, however, $\mathbf{\Omega}$ can be represented by its strength, which is a scalar property. Thus, $\mathbf{\Omega}^2=II_\Omega\mathbf{I}_2/2$, where $\mathbf{I}_2$ is the 2×2 identity matrix. This implies that $\mathbf{N}^\Omega=-\sqrt{-II_\Omega}\mathbf{a}$ for 2D mean flows. Hence, including $\mathbf{N}^\Omega$ for 2D mean flows, in principle becomes a matter of transforming N, see the next section. For 3D mean flows, on the other hand, the nonlinearity of $\mathbf{N}^\Omega$ cannot be represented by a scalar and requires the use of a tensor basis based on the three tensors $\mathbf{S}$, $\mathbf{\Omega}$ and $\mathbf{\Omega}^{(r)}$. This is an awkward solution to the problem since the resulting EARSM formulation would be very lengthy and of no practical use. This is further discussed in Section

3.5. A more tractable procedure is hence needed and by reformulating $\mathbf{N}^{\Omega}$ in terms of $\mathbf{\Omega}^*$ as

$$\mathbf{N}^{\Omega}_{\text{approx}} = \frac{\sqrt{-II_{\Omega}}}{-II_{\Omega^*}}\left(\mathbf{a}\mathbf{\Omega}^{*2} + \mathbf{\Omega}^{*2}\mathbf{a} - \frac{2}{3}\{\mathbf{a}\mathbf{\Omega}^{*2}\}\mathbf{I}\right) \tag{15}$$

(12) becomes solvable, in terms of N, for 2D and 3D mean flows when using the appropriate approximation of $\mathbf{N}^S$ for 3D mean flows (see below). Furthermore, the approximation (15) will in a consistent way reduce to the exact 2D formulation in case of 2D mean flows. Also, when the curvature correction is switched off, (15) reduces to its original form, (8). The adequacy of (15) as an approximation of (8) is discussed in Section 4.3.

3. EARSM formulation

To reach an EARSM formulation, (12) is solved by expanding the Reynolds stress anisotropy in terms of a tensor basis derived from the mean velocity gradients by using the Caley–Hamilton theorem. The algebraically least complex way to do this is in terms of a 10 element tensor basis, $\mathbf{T}^{(i)}$. The 10 basis tensors can, in fact, be reduced to five tensors, but the resulting coefficients will be extremely lengthy, see Taulbee et al. (1994). Thus, the Reynolds stress anisotropy is most conveniently expanded as

$$\mathbf{a} = \sum_{i=1}^{10} \beta_i \mathbf{T}^{(i)} \tag{16}$$

This expansion is then inserted into (12) and solved for the β-coefficients which can depend on the invariants of $\mathbf{S}$ and $\mathbf{\Omega}^*$

$$\begin{aligned} &II_S = \{\mathbf{S}^2\}, \quad II_{\Omega^*} = \{\mathbf{\Omega}^{*2}\}, \quad III_S = \{\mathbf{S}^3\} \\ &IV = \{\mathbf{S}\mathbf{\Omega}^{*2}\}, \quad V = \{\mathbf{S}^2\mathbf{\Omega}^{*2}\} \end{aligned} \tag{17}$$

The scalar nonlinearity in the unknowns (β-coefficients) on the left hand side of (12) is addressed by solving a polynomial equation for N after the β-coefficients have been determined from the linear set of equations where N is left as an additional unknown, see Wallin and Johansson (2000).

It has been shown, see e.g. Taulbee (1992), that for $A_2 = 0$ and $c = 0$, (12) maps to five basis tensors for 3D mean flows:

$$\begin{aligned} &\mathbf{T}^{(1)} = \mathbf{S}, \quad \mathbf{T}^{(3)} = \mathbf{\Omega}^{*2} - \frac{1}{3}II_{\Omega^*}\mathbf{I} \\ &\mathbf{T}^{(4)} = \mathbf{S}\Omega^* - \mathbf{\Omega}^*\mathbf{S} \\ &\mathbf{T}^{(6)} = \mathbf{S}\mathbf{\Omega}^{*2} + \mathbf{\Omega}^{*2}\mathbf{S} - \frac{2}{3}IV\mathbf{I} \\ &\mathbf{T}^{(9)} = \mathbf{\Omega}^*\mathbf{S}\mathbf{\Omega}^{*2} - \mathbf{\Omega}^{*2}\mathbf{S}\mathbf{\Omega}^* \end{aligned} \tag{18}$$

This is convenient since the model based on a full 10 tensor basis is much more complex, and the behaviour in terms of singularities is presently not known.

Since we are interested in the curvature corrected model formulation, $\mathbf{\Omega}^*$ rather than $\mathbf{\Omega}$ will be used in the basis tensors (18) and the invariants (17).

3.1. EARSM solution for 2D mean flows

In 2D mean flows the nonlinear terms reduce to $\mathbf{N}^{\Omega}_{\text{approx}} = \mathbf{N}^{\Omega} = -\sqrt{-II_{\Omega}}\mathbf{a}$ and $\mathbf{N}^S = \sqrt{II_S}\mathbf{a}$, and with $A_2 = 0$ and $c \neq 0$, the EARSM solution maps to $\mathbf{T}^{(1)}$ and $\mathbf{T}^{(4)}$. The corresponding β-coefficients are

$$\beta_1 = -\frac{A_1 N^*}{N^{*2} - 2II_{\Omega^*}}, \quad \beta_4 = -\frac{A_1}{N^{*2} - 2II_{\Omega^*}} \tag{19}$$

N^* is given by the physical solution of the third order equation

$$N^{*3} - A_3^* N^{*2} - (A_1 A_4 II_S + 2II_{\Omega^*})N^* + 2A_3^* II_{\Omega^*} = 0 \tag{20}$$

which is the same equation as for the baseline EARSM, Wallin and Johansson (2000), but with $N \to N^* = N - c(\sqrt{II_S} - \sqrt{-II_{\Omega}})$ and $A_3 \to A_3^* = A_3 - c(\sqrt{II_S} - \sqrt{-II_{\Omega}})$. Note that it is the inertial II_{Ω} that is used for the A_3^* relation. The physical solution of (20) is given by

$$N^* = \begin{cases} \frac{A_3^*}{3} + \text{sign}(P_1 + \sqrt{P_2})|(P_1 + \sqrt{P_2})|^{1/3} \\ \quad + \text{sign}(P_1 - \sqrt{P_2})|P_1 - \sqrt{P_2}|^{1/3}, \quad P_2 \geqslant 0 \\ \frac{A_3^*}{3} + 2(P_1^2 - P_2)^{1/6}\cos\left(\frac{1}{3}\arccos\left(\frac{P_1}{\sqrt{P_1^2 - P_2}}\right)\right), \\ \quad P_2 < 0, \ P_1 \geqslant 0 \\ \frac{A_3^*}{3} + 2(P_1^2 - P_2)^{1/6}\cos\left(-\frac{1}{3}\arccos\left(\frac{-P_1}{\sqrt{P_1^2 - P_2}}\right) + \frac{\pi}{3}\right), \\ \quad P_2 < 0, \ P_1 < 0 \end{cases} \tag{21}$$

where

$$P_1 = \left(\frac{A_3^{*2}}{27} + \frac{A_1 A_4}{6}II_S - \frac{2}{3}II_{\Omega^*}\right)A_3^* \tag{22}$$

$$P_2 = P_1^2 - \left(\frac{A_3^{*2}}{9} + \frac{A_1 A_4}{3}II_S + \frac{2}{3}II_{\Omega^*}\right)^3 \tag{23}$$

Negative values of P_1 must be considered in the solution for N^* due to the fact that A_3^* can attain negative values since $\text{sign}(A_3^*) = \text{sign}(P_1)$ according to (22). This means that N^* has the possibility to become negative. This should in general be avoided since it for 2D mean flows directly corresponds to having a negative production to dissipation rate, $\mathscr{P}/\varepsilon \equiv -\{\mathbf{a}\mathbf{S}\} = -\beta_1 II_S$ since $\beta_1 > 0$ for $N^* < 0$ according to (19). The easiest way to avoid this is to impose a lower limit to N^* such that $N^* \to \max(N^*, 0)$.

When $P_2 < 0$ this limit will not be activated since the N^*-solution, (21), cannot attain negative values. This can be seen from the third row of (21). A negative N^* can, as pointed out above, only happen if A_3^* and hence P_1 are negative. The cos-function will then return values >0.5. Furthermore, from (22) it is clear that $|P_1| \geqslant |A_3^{*3}|/27$. Assuming $A_3^* < 0$ ($P_1 < 0$) and $P_2 < 0$, this implies that

$$N^* = \frac{A_3^*}{3} + 2(P_1^2 - P_2)^{1/6}\cos(\cdots) > \frac{A_3^*}{3} + 2(P_1^2)^{1/6}\frac{1}{2} \geqslant -\frac{|A_3^*|}{3} + \left(\frac{|A_3^*|^6}{27^2}\right)^{1/6} = 0. \quad (24)$$

In other words, $N^* > 0$ in the whole parameter region $P_2 < 0$.

When $P_2 \geqslant 0$, on the other hand, putting zero as the lower limit on N^*, directly corresponds to implying a zero lower limit to A_3^*.

Negative production is not feasible in algebraic Reynolds stress modelling, although it is physically possible. A lower limit on N^* is indeed ad hoc, but is needed in order to avoid numerical problems in the iteration procedure. The parameter regime where the limit is active is associated with vanishing or negative production. The weak equilibrium assumption is not valid here and a limit in order to avoid spurious solutions can be justified. Moreover, this parameter regime is rarely reached and it should be pointed out that it is not present in the test cases discussed below.

3.2. EARSM solution for 3D mean flows

For 3D mean flows the representation of the nonlinear tensor $\mathbf{N}^S$ in the five element basis (18) is extremely complex (see Appendix A). In order to eliminate this problem $\mathbf{N}^S$ can be approximated with its exact expression in 2D mean flows, $\mathbf{N}^S_{2D} = \sqrt{II_S}\mathbf{a}$. This approximation is further discussed in Section 4.3.

With $A_2 = 0$, $\mathbf{N}^S = \sqrt{II_S}\mathbf{a}$ and the addition of the nonlinear contribution $\mathbf{N}^\Omega$ in (15) the corresponding EARSM coefficients become

$$\begin{aligned}
\beta_1 &= A_1(N^*c^2II_\Omega + 8cII_{\Omega^*}\sqrt{-II_\Omega} - 14N^*II_{\Omega^*} + 4N^{*3})/(Q_1Q_2)\\
\beta_3 &= 4IVA_1(2c^2II_\Omega N^{*2} + c^3N^*(-II_\Omega)^{3/2} - 18II^2_{\Omega^*}\\
&\quad + 18cN^*\sqrt{-II_\Omega}II_{\Omega^*} + 7c^2II_{\Omega^*}II_\Omega)\\
&\quad /(II^2_{\Omega^*}(2c\sqrt{-II_\Omega} - 3N^*)Q_1Q_2)\\
\beta_4 &= 4A_1/Q_1\\
\beta_6 &= -2A_1(N^*c^2II_\Omega + 4cII_{\Omega^*}\sqrt{-II_\Omega}\\
&\quad + 2N^{*2}c\sqrt{-II_\Omega} - 6N^*II_{\Omega^*})/(II_{\Omega^*}Q_1Q_2)\\
\beta_9 &= 2A_1(4cN^*\sqrt{-II_\Omega} + c^2II_\Omega - 6II_{\Omega^*})/(II_{\Omega^*}Q_1Q_2)
\end{aligned} \quad (25)$$

where

$$\begin{aligned}
Q_1 &= -(2N^* - c\sqrt{-II_\Omega})^2 + 2II_{\Omega^*}\\
Q_2 &= N^{*2} - 2II_{\Omega^*}
\end{aligned} \quad (26)$$

The equation for N^* for 3D mean flows is a very lengthy sixth order equation that will not be given here. This equation is of little practical use. Here we instead us the cubic equation (20) for both 2D and 3D mean flows. Improvements of N^* are discussed in Section 4.3.

3.3. The inclusion of terms nonlinear in the Reynolds stress anisotropy

We also made an attempt of including a term, $\mathbf{G}$, nonlinear in the Reynolds stress anisotropy tensor in the pressure strain rate model (7). $\mathbf{G} = \mathbf{a}^2\mathbf{\Omega} - \mathbf{\Omega}\mathbf{a}^2$ is one of the terms in the most general model linear in $\mathbf{S}$ and $\mathbf{\Omega}$ (see e.g. Johansson and Hallbäck, 1994). For 2D mean flows the inclusion of $\mathbf{G}$ in the pressure strain rate model will not change the EARSM solution if $A_2 = 0$. This can be explained by the fact that for the particular choice of $A_2 = 0$, the normal anisotropy component in the third direction vanishes in 2D mean flows, and thus, also $\mathbf{G}$ vanishes. For 3D mean flows the contribution of $\mathbf{G}$ does not vanish in general. This is independent of the A_2-coefficient. Instead the nonlinear nature of the term gives an ARSM-relation which consists of a system of coupled quadratic equations in the five unknowns. The complexity of the system of equation leaves very little hope of finding an analytical solution. Thus, the problem will not be further discussed here.

The widely used SSG-model proposed by Speziale et al. (1991) contains the term $\mathbf{G}_{\mathbf{a}^2} = \mathbf{a}^2 - \frac{1}{3}II_\mathbf{a}\mathbf{I}$. The inclusion of this term gives an ARSM relation which consists of a system of nonlinear equations. For 2D mean flows, this term can, in principal, be included in an EARSM approach. Three basis tensors are needed since $\mathbf{a}^2$ directly maps to $\mathbf{T}^{(2)}$ when $\mathbf{T}^{(1)}$ is squared. The nonlinear dependency between the β-coefficients can be reduced to a fourth order polynomial equation for one of the β-coefficients. Although this can be solved analytically, the solution will be lengthy and the problem of finding the correct root of the equation for N is not easily solved. Therefore, no further work on this is presented here. For 3D mean flows, the inclusion of $\mathbf{G}_{\mathbf{a}^2}$ gives an ARSM-relation which constitutes a system of nonlinear equation to which no analytical solution can be found.

3.4. Recalibration of A_0

In the basic curvature corrected model by Wallin and Johansson (2002), WJ-EARSM, the A_0-coefficient was calibrated considering homogeneous rotating shear. By arguing that the model should be neutrally stable for rotation number $Ro = 1/2$, where $Ro \equiv \omega_z^{(r)}/(\mathrm{d}U/\mathrm{d}y)$, the value $A_0 = -0.72$ was obtained (see Wallin and Johansson, 2002 for details). Since we are adding additional terms, $\mathbf{N}^\Omega$ and $\mathbf{N}^S$, that contribute in rotating flows, the value of A_0 needs to be recalibrated in order to preserve neutral stability for $Ro = 1/2$.

Wallin and Johansson (2002) obtained the A_0-value by considering the standard K–ε platform (see Appendix B) with parameter values $C_{\varepsilon 1} = 1.44$ and $C_{\varepsilon 2} = 1.83$. A perhaps more natural choice would be to calibrate the model against the standard K–ω platform, Wilcox

(1988), since it is used in all wall bounded test cases of this work. This is however a choice, and not a necessity. The standard K–ω platform parameter values are $\alpha = 5/9$, $\beta = 3/40$ and $\beta^* = 0.09$. For homogeneous flows this is equivalent to a K–ε platform with the parameters, $C_{\varepsilon 1} = \alpha + 1 = 1.56$ and $C_{\varepsilon 2} = \beta/\beta^* + 1 = 1.83$. The corresponding value for the WJ-EARSM is $A_0 = -0.70$. The authors feel that this can be considered as an alternative calibration of A_0.

For the present model, an analytical relation for the model coefficients cannot be derived, as was done by Wallin and Johansson for the basic model without the nonlinear terms. Instead, the A_0-coefficient was adjusted such that the computed turbulent kinetic energy initially will evolve as for the WJ-EARSM with $A_0 = -0.70$ together with the standard K–ω platform. That resulted in $A_0 = -0.9$ which is used in the following. The computed evaluation of K for the neutrally stable case used for the calibration is shown in Fig. 1c.

3.5. Remark on alternative projection methods

One can argue that the choice of the approximation of the $\mathbf{N}^{\Omega}$ term given by (15) is not unique and somewhat ad hoc. A formally more correct way of obtaining an expression for $\mathbf{N}^{\Omega}$ in terms of the $\mathbf{S}$ and $\mathbf{\Omega}^*$ tensors, would be to project it onto the tensor basis (18) using the procedure outlined by for instance Jongen and Gatski (1998). This procedure which is based on the least square method, provides a formal way of representing a tensor in terms of any appropriate tensor basis. It is not only possible to exactly solve (5) by using a complete tensor basis, but also to directly project the solution on an incomplete tensor basis. This new representation would be the optimal in a least square sense.

If we let the representation of $\mathbf{N}^{\Omega}$ be denoted by $\mathbf{N}^{\Omega}_P$ then it is guaranteed that $\|\mathbf{N}^{\Omega} - \mathbf{N}^{\Omega}_P\|$ is minimal where the norm $\|\cdot\|$is defined as

$$\|\mathbf{X}\|^2 \equiv X_{mn}X_{mn} \tag{27}$$

and for a symmetric tensor $\|\mathbf{X}\|^2 = \{\mathbf{X}^2\}$ holds. The expression for $\mathbf{N}^{\Omega}_P$ becomes

$$\mathbf{N}^{\Omega}_P = \sum_{i=1,3,4,6,9} \frac{\alpha_i}{\alpha_0}\mathbf{T}^{(i)} \tag{28}$$

and where $\alpha_i = \det(\mathbf{D}^{(i)})$ and $\mathbf{D}^{(i)}$ are 5×5 matrices given by

$$D^{(i)}_{kl} = \begin{cases} \{\mathbf{T}^{(l)}\mathbf{T}^{(k)}\}, & l \neq i \\ \{\mathbf{N}^{\Omega}\mathbf{T}^{k}\}, & l = i \end{cases} \tag{29}$$

Since the five-term basis (18) is complete, $\mathbf{N}^{\Omega}$ will be exactly represented by $\mathbf{N}^{\Omega}_P$. The amount of algebra generated with this approach is extensive. For instance, α_0 will be a polynomial of the invariants of $\{\mathbf{S}, \mathbf{\Omega}^*\}$ while α_i $i \neq 0$ would be polynomials of traces of tensor products of $\{\mathbf{a}, \mathbf{S}, \mathbf{\Omega}, \mathbf{\Omega}^*\}$ (see Appendix A for details). The numerical behaviour of the αs may therefore be very dif-

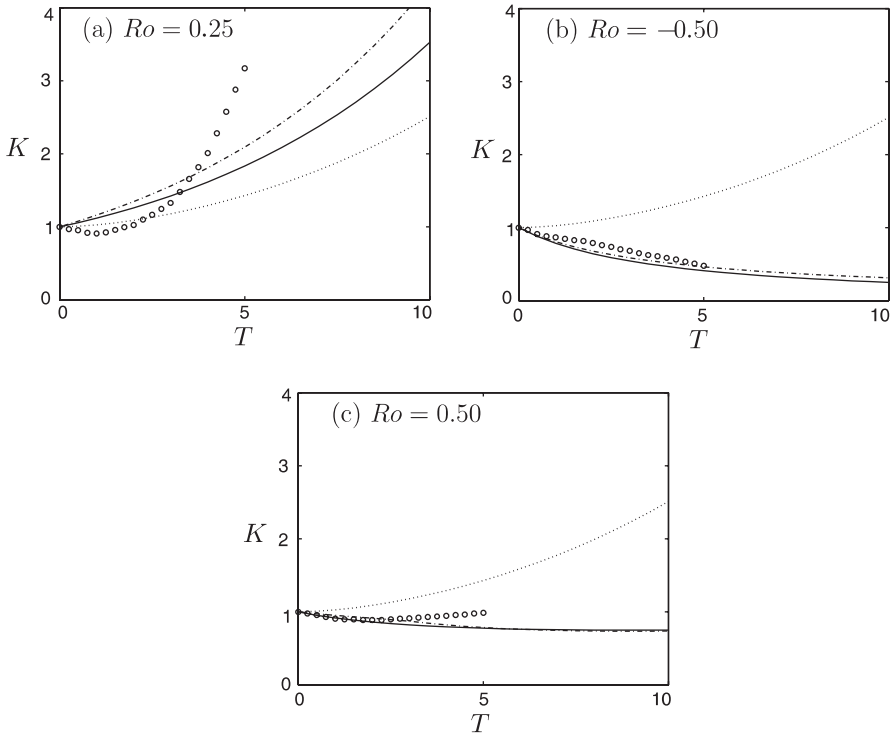

Fig. 1. Rotating homogeneous shear flow, $\mathrm{d}U/\mathrm{d}y = 3.4$. Proposed model (-·), WJ-EARSM (—), eddy-visc (···) compared to the large eddy simulation (LES) by Bardina et al. (1983) (○).

ficult to handle in terms of singularities. Moreover, since the α-coefficients will be functions of the different invariants involving the anisotropy, the equation for N will not be retained.

The same procedure can of course be applied to $\mathbf{N}^S$, (9). Although the algebra here will be somewhat simplified since $\mathbf{\Omega}$ does not have to be dealt with, the final form of the EARSM will be extremely lengthy and of limited practical use (see Appendix A).

To reduce the complexity, an incomplete tensor basis using fewer elements can be used. The representation would although not being exact, be optimal in a least square sense, see Appendix A for details. However, by using an incomplete basis the final expression will be dependent in the choice of the tensor basis. Moreover, there is also a certain degree of freedom in the definition of the norm. In all, this will prevent us from reaching the original goal of eliminating as many ad hoc assumptions or approximations as possible.

4. Test cases

The proposed model has been tested for three generic flows: rotating homogeneous shear flow and rotating channel flow with 2D mean flows and rotating pipe flow where the mean flow is 3D. Comparisons have been made with LES by Bardina et al. (1983) for the rotating homogenous shear flow, DNS by Alvelius (1999) for the channel flow and experimental data by Imao et al. (1996) for the rotating pipe flow.

The curvature correction was used in all computations implying the appropriate use of $\mathbf{\Omega}^*$, as defined in (14). For the proposed EARSM, the model parameters were $A_0 = -0.9$ and $C_\Omega = 0.5$ as proposed by Sjögren and Johansson (2000), which yields $c = -C_\Omega/A_0 = 0.56$. Furthermore $A_1 = 1.20$, $A_2 = 0$, $A_3 = 1.80$ and $A_4 = 2.25$, see Wallin and Johansson (2002). The WJ-EARSM corresponds to $c = 0$ and $A_0 = -0.72$ as originally proposed by Wallin and Johansson (2002) except for the rotating homogeneous rotating shear flow case where $A_0 = -0.70$ has been used for calibration purposes as discussed in Section 3.4. It should further be pointed out that rotating channel and rotating pipe flow have been computed using WJ-EARSM with both $A_0 = -0.70$ and -0.72. The differences were, however, unsignificant.

The diffusion model proposed by Daly and Harlow (1970) has been used to model the diffusion of the quantities in the platform equations, see Appendix B for details.

4.1. 2D mean flow: homogeneous rotating shear flow

Homogenous rotating shear was computed for three different rotation numbers $Ro \equiv \omega_z^{(r)}/(\mathrm{d}U/\mathrm{d}y)$ of 1/4, 1/2 and $-1/2$ using the K–ε platform together with the proposed model, the WJ-EARSM and an eddy viscosity model. For details on the K and ε equations, see Appendix B. Note, however, that for this homogeneous flow case, the K–ε and K–ω two-equation platforms are equivalent.

Fig. 1a shows the development of the turbulence kinetic energy for the most energetic case, $Ro = 1/4$. As can be seen the inclusion of the nonlinear terms increases the growth rate. K is, however, still underpredicted compared to the long time behaviour of the Bardina LES. The stable case with $Ro = -1/2$ is shown in Fig. 1b. Predictions of both the WJ-EARSM and the proposed model agree well with the Bardina LES data. The neutrally stable case of $Ro = 1/2$ is shown in Fig. 1c. The change in the turbulence kinetic energy is small and the agreement with the Bardina LES good, as expected, since the A_0-coefficient was calibrated for capturing the neutrally stable case.

4.2. 2D mean flows: fully developed rotating channel flow

The second 2D mean flow test case is a fully developed rotating channel flow. The channel coordinate system $\{\mathbf{e}_x, \mathbf{e}_y, \mathbf{e}_z\}$ is rotating with the rate $\omega_z^{(r)}$ in the $\mathbf{e}_z$ direction. Computations were performed for two different rotation numbers, $Ro \equiv 2\omega_z^{(r)}\delta/U_m$, $Ro = 0.43$ and $Ro = 0.77$, see Fig. 2. The Reynolds number for the computation was $Re_\tau \equiv u_\tau\delta/\nu = 180$ where δ is the half channel width and $u_\tau^2 = \left((u_\tau^{\mathrm{s}})^2 + (u_\tau^{\mathrm{u}})^2\right)/2$ where u_τ^{s} and u_τ^{u} are the stable and unstable side friction velocities, respectively. Comparisons were made with the DNS data by Alvelius and the WJ-EARSM. The K–ω platform, see Appendix B, was used for both models.

The predictions of U^+ with the proposed model are somewhat improved, but still overestimated, see Fig. 2a and b. This effect is more prominent for the higher rotation number. The predictions of $\overline{uv}^+$ are almost unaffected, Fig. 2b. Both models lack the ability to correctly capture the small amount of positive shear stress on the stable side of the $\overline{uv}^+$ profile. A small amount of positive $\overline{uv}^+$ is predicted by both EARSMs for $Ro = 0.43$. The proposed model is somewhat closer to the DNS data. This effect is very small however.

The shortcomings of the near wall predictions of both models can to some extent be expected to depend on the choice of near-wall treatment in the EARSM and the platform equations. The high-Re form of the K–ω model is well known to give a too low value of the near wall peak of e.g. K.

4.3. 3D mean flows: rotating pipe flow

Fully developed flow in a circular pipe rotating around its symmetry axis is a suitable test case since it represents a three-dimensional mean flow that is dependent on only

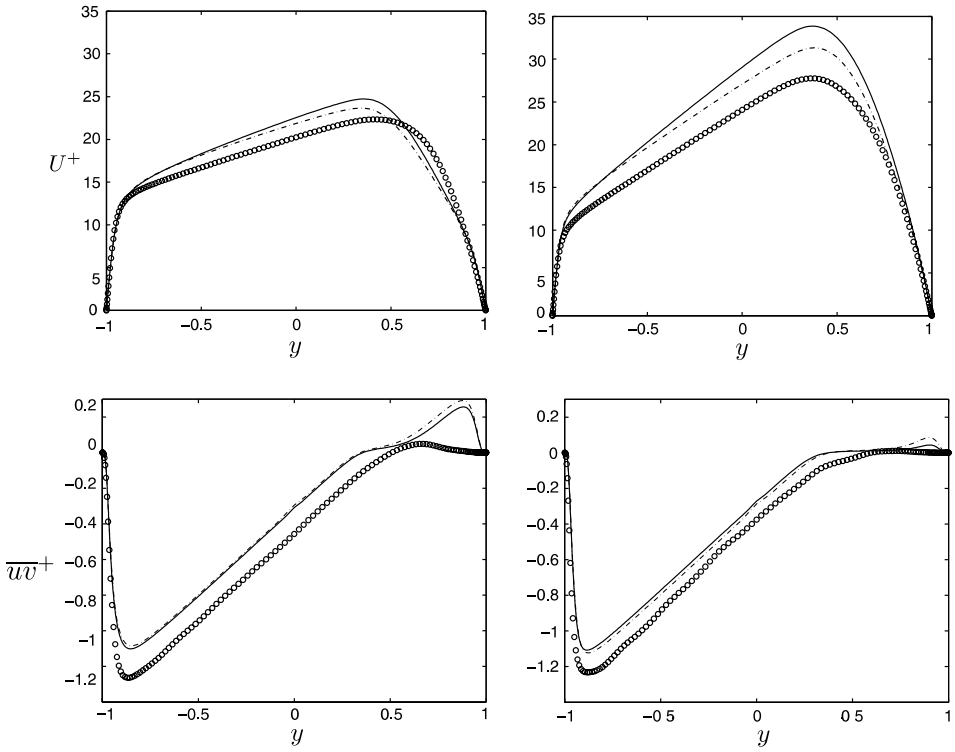

Fig. 2. Predicted velocity (upper) and turbulent shear stress (lower) of rotating channel flow for $Re_\tau = 180$ at $Ro = 0.43$ (left), $Ro = 0.77$ (right). Proposed EARSM (-·), WJ-EARSM (—) compared to DNS data by Alvelius (○).

one spatial coordinate, r. For a laminar rotating flow the tangential velocity, U_θ, varies linearly with the radius, r, while in case of turbulence U_θ has a parabola-like profile. This is indicated by the form of the integrated Reynolds equation in the tangential direction

$$U_\theta(r) = U_\theta(R)\frac{r}{R} - \frac{r}{v}\int_r^R \frac{Ka_{r\theta}}{r'}\,\mathrm{d}r' \tag{30}$$

where the first term corresponds to the linear variation with r and the second terms forces the U_θ-profile to a parabola-like shape through $a_{r\theta}$. Eddy-viscosity models as well as quadratic EARSMs (2D truncations) are unable to describe this phenomenon. Actually, a fully three-dimensional EARSM containing cubic terms is needed.

The proposed model has been used to compute rotating pipe flow at Reynolds number 20,000, based on the axial bulk velocity and the pipe diameter. Three different rotation rates were used, $Z = 0$, 0.5 and 1 where $Z = U_\theta(R)/U_m$, i.e. the wall tangential velocity divided by the axial bulk velocity. For $Ro = 1$, the proposed model had convergence problems. Comparisons are made with the WJ-EARSM and the K–ω model was used as model platform, see Appendix B.

To achieve convergence, a correction to N^* had to be applied. The correction provides a systematic improvement of the approximation of N^* for 3D mean flows and was derived by Wallin and Johansson (2000) and is described in the section below. This gives an indication on that the convergence problems for $Z = 1$ is due to the approximation of N^*. An observation that strengthens this argument is that if II_Ω is changed to II_{Ω^*} in the expression for A_3^*, convergence is also reached. The latter is of course somewhat ad hoc. But it still demonstrates that the approximation of N^* plays a determining role. For completeness, computations have been performed with and without the 3D correction of N^* for all the rotation rates.

Figs. 3 and 4 show the computed axial velocities compared with experimental data. For $Z = 0$, Fig. 3, both models predict a U_z that is somewhat too flat in the center of the pipe compared to the experimental data. This is due to the neglection of diffusion in the EARSM approximation, Wallin and Johansson (2000). For $Z = 0.5$, Fig. 4, the nonlinear terms have a positive effect on the predictions and the proposed model is in somewhat better agreement with the experimental data than the WJ-EARSM. Although the influence of the N-correction is small for this rotation number, it slightly improves the predictions of the WJ-EARSM. The proposed model, on the other hand, performs slightly worse with the correction applied. For $Z = 1$, Fig. 4, the WJ-EARSM is radically improved when the N^*-correction is applied. The proposed model (with correction) predicts an axial velocity that is somewhat too large in the center of the pipe. The shape of the profile is however better than that of the WJ-EARSM (with correction).

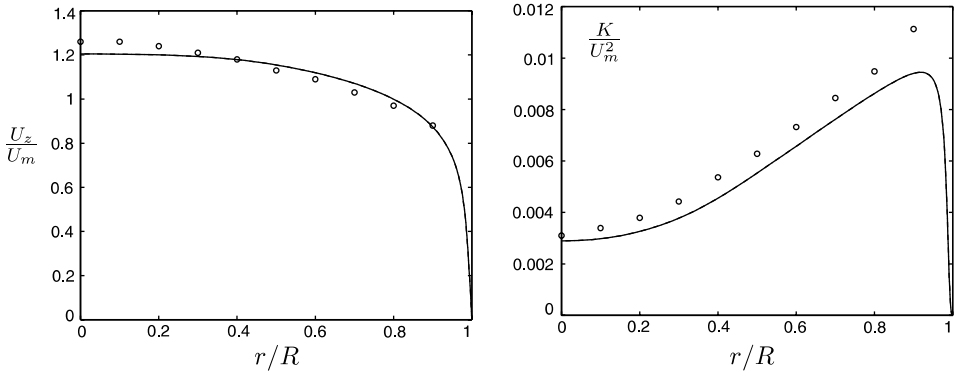

Fig. 3. Computed nonrotating pipe flow. Proposed EARSM and WJ-EARSM (—) (coinciding) compared to experimental data by Imao et al. (○).

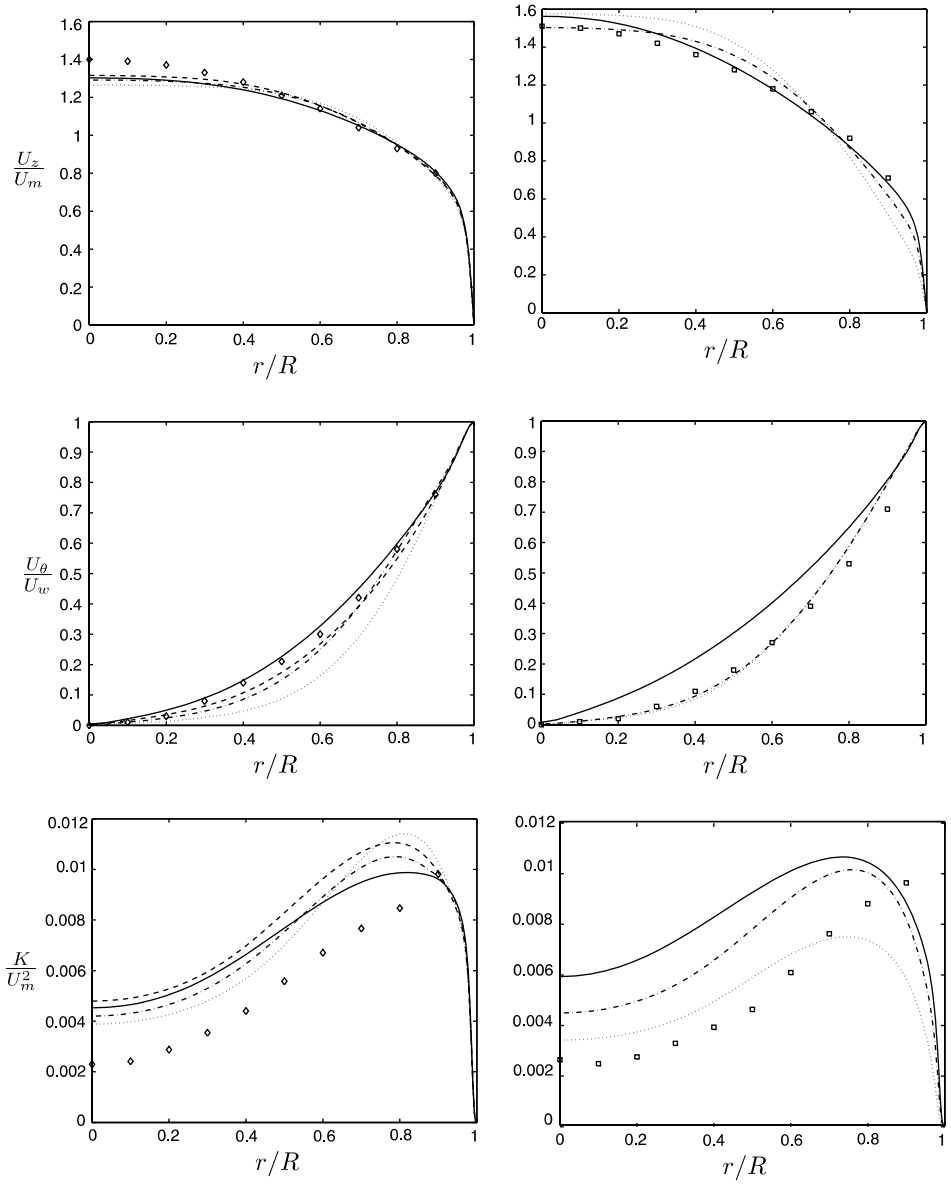

Fig. 4. Computed rotating pipe flow for $Z = 0.5$ (left) and $Z = 1$ (right). Proposed EARSM with (—) and without (– –) (N_{corr}), WJ-EARSM with (-·) and without (···) (N_{corr}). Experimental data by Imao et al. (symbols).

The tangential velocity profiles are shown in Fig. 4 (middle). For $Z = 0.5$, the proposed model clearly shows an improvement over the WJ-EARSM when the N^*-correction is not applied and the predicted U_θ agrees well with the experiments. With the correction applied the shape of the U_θ-profile is somewhat better with the proposed model. The overall deviation from solid body rotation is basically the same though. For $Z = 1$, the proposed model is too flat and the corrected and non-corrected forms of the WJ-EARSM closely resemble each other and agree well with the experiments.

The model predictions of the turbulence kinetic energy are compared with the experiment. Generally, the peak in K close to the wall is somewhat too small and too far from the wall. This can, to some extent, be attributed to the near wall treatment in the model platform. Furthermore, the turbulence level in the center of the pipe overpredicted for all tested models and rotation rates. The proposed model generally predicts higher turbulence levels than the WJ-EARSM. The N^*-correction also raises the turbulence levels, especially for $Z = 1$.

4.3.1. Achieving convergence for Z = 1

The convergence problems of the proposed model for $Z = 1$ are likely to depend on the use of the 2D mean flow form of N^* which means that the $\mathscr{P}/\varepsilon$ that corresponds to the 2D form of N^* is not fully consistent with the $\mathscr{P}/\varepsilon$ evaluated from the predicted anisotropy. The effects of a 3D mean flow become stronger with increasing rotation as pointed out above. This can, however, be overcome by applying a correction derived by Wallin and Johansson (2000). The idea is to do a linear extrapolation from the 2D mean N^*-solution for 3D mean flows. This is done by perturbing the IV and V invariants around the two-dimensional solution, that is $IV = \sqrt{\phi_1}$ and $V = II_S II_{\Omega^*} + \phi_2$, assuming that ϕ_1 and ϕ_2 are independent. ϕ_1 and ϕ_2 are zero in 2D mean flows. Using the correction implies that N^*, (21), in the β-coefficients is replaced by N_{3d} according to

$$N^* \Rightarrow N_{3\mathrm{D}} = N^* + N_{\mathrm{corr}} \tag{31}$$

where

$$N_{\mathrm{corr}} = \frac{162(\phi_1 + \phi_2 N^{*2})}{D} \tag{32}$$

and D is the denominator given by

$$D = 20N^{*4}\left(N^* - \frac{1}{2}A_3^*\right) - II_{\Omega^*}(10N^{*3} + 15A_3^* N^{*2}) + 10A_3^* II_{\Omega^*}^2 \tag{33}$$

D can be shown to be strictly positive and hence the correction should not add any numerical difficulties in terms of singularities, see Wallin and Johansson (2000).

The same procedure used by Wallin and Johansson (2000) for deriving the correction (31), can in principle also be applied to the proposed model to derive the corresponding correction for 3D mean flows. It turns out however that this is not a feasible approach since the governing sixth order equation for N^* is very complex. In this sense the correction is not a strict mathematic offspring of the sixth order equation for N^*. But still, it should be recognized as systematic improvement of the evaluation of N^* due to the fact that it is formally derived from the parent model of the proposed EARSM.

4.3.2. The approximations of $\mathbf{N}^{\Omega}$ and $\mathbf{N}^{S}$

Although being exact for 2D mean flows, the approximations of the nonlinear terms (8) and (9), $\mathbf{N}^{\Omega}_{\mathrm{approx}}$ and $\mathbf{N}^{S}_{\mathrm{2D}}$ respectively, are still only approximations in 3D mean flows. A natural way to quantify how large the differences are between the original forms and the approximations, is to study the normalized square root of the error defined by

$$E^x = \sqrt{\frac{\{(\mathbf{N}^x - \mathbf{N}^x_{\mathrm{approx}})^2\}}{\{\mathbf{N}^{x2}\}}} \tag{34}$$

Note that $\mathbf{N}^{S}_{\mathrm{approx}} = \mathbf{N}^{S}_{\mathrm{2D}}$. Both N^x and N^x_{approx} are evaluated from a given solution. This provides an invariant scalar measure of the difference or error between the tensor x and its approximation. It is necessary to take the square since these terms are part of the pressure strain modelling and hence are traceless. This is also in general

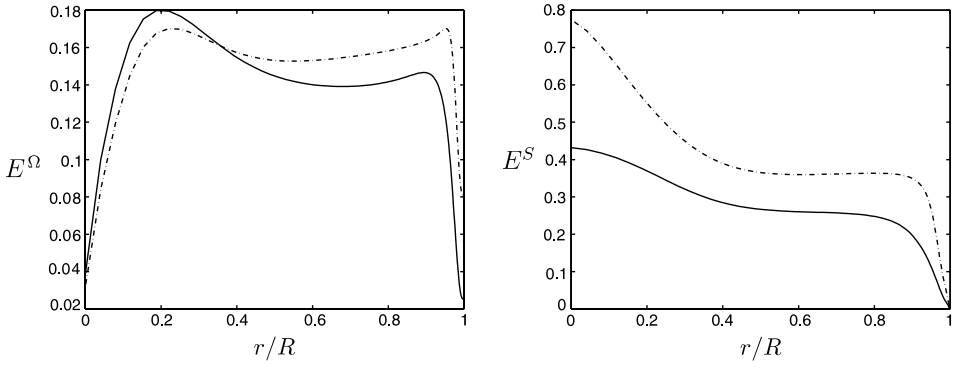

Fig. 5. E^{Ω} (left) and E^{S} (right) for $Z = 0.5$ (—) and $Z = 1$ (-·).

agreement with the concept of studying least squares in Appendix A.

In Fig. 5, E^{Ω} and E^{S} are shown for $Z = 0.5$ and $Z = 1$ using the mean flow, K and ω-values of the WJ-EARSM in conjunction with the N-correction. For $Z = 0$, the approximations are exact, as discussed earlier, and no differences occur. As an approximation $\mathbf{N}^{\Omega}_{\text{approx}}$ performs significantly better than $\mathbf{N}^{S}_{\text{2D}}$, especially for the case with higher rotation. This should be expected since $\mathbf{N}^{S}_{\text{2D}}$ is the 2D mean flow form of $\mathbf{N}^{S}$. One should keep in mind, however, that the largest values ($\geqslant 50\%$ of the maximum value) of $\mathbf{N}^{S}$ are attained in the region $0.4 \leqslant r \leqslant 0.9$. In the center of the pipe, $\mathbf{N}^{S}$ is zero, simply because of a zero mean velocity gradient. Therefore, the effect of the relatively high values of E^{S} in center of the pipe should not be overestimated.

5. Concluding remarks

The differential Reynolds stress model by Sjögren and Johansson (2000), SJ-DRSM, was derived by permitting tensor terms, nonlinear in the anisotropy, in the modelling of the rapid pressure strain. In this way, sufficient degree of freedom was obtained in order to impose constraints, such as realizability and correct behaviour in the rapid distortion limit. Including these terms in a DRSM is fairly straight forward. For an EARSM, on the other hand, the nonlinearities lead to systems of nonlinear equations which might have different properties for 2D and 3D mean flows. For instance, $\mathbf{G} = \mathbf{a}^2\boldsymbol{\Omega} - \boldsymbol{\Omega}\mathbf{a}^2$ have been shown to vanish for 2D mean flows for the specific choice of $A_2 = 0$, while for 3D mean flows a system of nonlinear equations is obtained. No general way of including terms nonlinear in the anisotropy into an EARSM framework could be found.

Sjögren and Johansson also proposed terms, $\mathbf{N}^{\Omega}$ and $\mathbf{N}^{S}$, linear in the Reynolds stress anisotropy tensor with a quadratic tensorial dependence on the mean velocity gradients. These terms were chosen in order to improve the predictions of a number of rotating flows and selected on a somewhat ad hoc and less formal basis. Still, they were shown to have significant effect on the predictions of a number of rotating flows. From an EARSM point of view, these contributions are more appealing since they are linear in the Reynolds stress anisotropy, and hence, preserves the quasi-linearity of the ARSM equation.

Although $\mathbf{N}^{\Omega}$ and $\mathbf{N}^{S}$ can be included in a formally correct way, the representations of $\mathbf{N}^{\Omega}$ and $\mathbf{N}^{S}$ in terms of the five element tensor basis (18) are very lengthy and the solution to the ARSM equation for 3D mean flows are too complicated to be of practical importance. For 2D mean flows the new terms can be fully accounted for since they merely give a change of the model coefficient A_3. Different approximations of $\mathbf{N}^{\Omega}$ and $\mathbf{N}^{S}$ have been considered, that are consistent with the original form in 2D mean flows, but where the complexity in 3D mean flows is reduced. The suggested approximations provide formulations that can be easily incorporated in a consistent EARSM formulated in conjunction with curvature corrections derived from the advection of the Reynolds stress anisotropy. The full 3D representation, although it contains approximations, is important for capturing secondary flows generated by the Reynolds stress anisotropy. Judging from the discussion in Section 4.3.2, one can argue that the errors of these approximations are relatively large, especially in flows where the effects of a 3D mean flow are strong. This seems, however, to be inevitable if the effects of tensorial nonlinear modelling based on the mean velocity gradients are to be included in a relatively compact EARSM formulation based on a complete tensor basis.

The proposed model has been tested for a number of generic flows where the effects of rotation are strong. For the 2D mean flow cases, homogeneous rotating shear and rotating channel flow, an over all improvement can be seen. For the rotating channel, however, the improvements are very small and not universal. For the rotating pipe case, the mean velocity profiles are in good qualitative agreement with experimental data. The nonlinear contributions have been shown to have a positive contribution to the overall shape of the mean axial velocity which is important from an engineering point of view. The predicted mean azimuthal velocity profile is somewhat flatter for the proposed model than for the WJ-EARSM. This implies good agreement with the experiments for $Z = 0.5$. For $Z = 1$, the profile is too flat. The turbulence intensities are generally overpredicted compared to experiments and significantly higher than for the WJ-EARSM for the case with highest rotation. The convergence problem occurring for this model for $Z = 1$, have been demonstrated to be related to the approximation of N. This can, however, be overcome by adding a correction to N. In a separate work, the proposed model was implemented in a "production" CFD code and shown to give good predictions and to be robust when applied to e.g. high-lift aerodynamics applications for both 2D and 3D mean flows.

Acknowledgements

This work has been carried out within the HiAer project (High Level Modelling of High Lift Aerodynamics). The HiAer project is a collaboration between DLR, ONERA, KTH, HUT, TUB, Alenia, Airbus-D, QinetiQ and FOI. The project is managed by FOI and is partly funded by the European Union (Project Ref: G4RD-CT-2001-00448).

Appendix A. Projections of $\mathbf{N}^{\Omega}$ and $\mathbf{N}^{S}$ onto a five element tensor basis

While the suggested approximation of $\mathbf{N}^{\Omega}$, (15), is consistent for 2D and 3D mean flows and can easily be incorporated in EARSM formulated in terms of the five element tensor basis (18), it is somewhat ad hoc and its uniqueness not guaranteed. A formally more correct procedure would be to represent $\mathbf{N}^{\Omega}$ in terms of the chosen tensor basis in such a way that the difference between the representation, $\mathbf{N}_r^{\Omega}$ say, and $\mathbf{N}^{\Omega}$ is minimal. Such a formulation can be achieved by minimizing $\|\mathbf{N}^{\Omega}-\mathbf{N}_r^{\Omega}\|$ in a least square sense using the norm $\|\cdot\|$. However, one needs to be aware of the fact that for this method there is a certain degree of freedom, like the choice of tensor basis and the definition of the norm.

This procedure has been used earlier by for instance Jongen and Gatski (1998), see also Gatski and Jongen (2000), to derive representations of tensors in terms of a given tensor basis, but also to derive explicit algebraic Reynolds stress models from the ARSM relation (5). The approach described is attractive in the sense that it provides a formal way to represent any tensor in terms of an appropriate tensor basis. Below, the essential steps of the procedure will be described briefly and then the corresponding representation of $\mathbf{N}^{\Omega}$ and $\mathbf{N}^{S}$ in the five element basis will be shown. For a more thorough discussion on the above procedure and related topics see, for instance, Jongen and Gatski (1998) or Gatski and Jongen (2000).

Assuming that we have N linearly independent basis tensors $\{\mathbf{T}^{(1)},\ldots,\mathbf{T}^{(N)}\}$ the representation of $\mathbf{N}^{\Omega}$ is expressed as

$$\mathbf{N}_r^{\Omega}=\sum_{n=1}^{N}c_n^{\Omega}\mathbf{T}^{(n)} \tag{35}$$

Using a norm defined as

$$\|\mathbf{X}\|^2\equiv X_{mn}X_{mn}=\{\mathbf{X}^2\} \tag{36}$$

where $\mathbf{X}$ is a symmetric tensor, minimizing $\|\mathbf{N}^{\Omega}-\mathbf{N}_r^{\Omega}\|^2$ corresponds to minimizing

$$\begin{aligned}E(c_1^{\Omega},\ldots,c_N^{\Omega})&=\|\mathbf{N}^{\Omega}-\mathbf{N}_r^{\Omega}\|^2\\&=\|\mathbf{N}^{\Omega}\|^2+\sum_{n=1}^{N}\sum_{m=1}^{N}c_n^{\Omega}c_m^{\Omega}\{\mathbf{T}^{(n)}\mathbf{T}^{(m)}\}\\&\quad-2\sum_{N=1}^{N}c_n^{\Omega}\{\mathbf{N}^{\Omega}\mathbf{T}^{(n)}\}\end{aligned} \tag{37}$$

with respect to $\{c_1^{\Omega},\ldots,c_N^{\Omega}\}$. This gives

$$\begin{aligned}&\frac{\partial E}{\partial c_m^{\Omega}}=0=2\sum_{n=1}^{N}c_n^{\Omega}\{\mathbf{T}^{(n)}\mathbf{T}^{(m)}\}-2\{\mathbf{N}^{\Omega}\mathbf{T}^{(m)}\},\\&m=1,\ldots,N\end{aligned} \tag{38}$$

$$\begin{aligned}&\Rightarrow\ \sum_{n=1}^{N}c_n^{\Omega}\{\mathbf{T}^{(n)}\mathbf{T}^{(m)}\}=\{\mathbf{N}^{\Omega}\mathbf{T}^{(m)}\},\\&m=1,\ldots,N\end{aligned} \tag{39}$$

which is a system of N linear equations in the unknowns $\{c_1^{\Omega},\ldots,c_N^{\Omega}\}$. Note here that c_i^{Ω} corresponds to α_i/α_0 in (28) where $\{\alpha_i\}$ are computed using Cramer's rule.

In our case we would like to represent $\mathbf{N}^{\Omega}$ in terms of the five element tensor basis

$$\begin{aligned}\mathbf{T}^{(1)}&=\mathbf{S},\quad \mathbf{T}^{(2)}=\boldsymbol{\Omega}^{*2}-\frac{1}{3}II_{\Omega^*}\mathbf{I},\\\mathbf{T}^{(3)}&=\mathbf{S}\boldsymbol{\Omega}^{*}-\boldsymbol{\Omega}^{*}\mathbf{S},\\\mathbf{T}^{(4)}&=\mathbf{S}\boldsymbol{\Omega}^{*2}+\boldsymbol{\Omega}^{*2}\mathbf{S}-\frac{2}{3}IV\mathbf{I},\\\mathbf{T}^{(5)}&=\boldsymbol{\Omega}^{*}\mathbf{S}\boldsymbol{\Omega}^{*2}-\boldsymbol{\Omega}^{*2}\mathbf{S}\boldsymbol{\Omega}^{*}\end{aligned} \tag{40}$$

Note here that (40) corresponds to (18), but with the numbers changed in order to match (35). Since (40) is complete it follows that $\mathbf{N}_r^{\Omega}=\mathbf{N}^{\Omega}$. Solving (39) for $\{c_1^{\Omega},\ldots,c_N^{\Omega}\}$, using

$$\mathbf{N}^{\Omega}=\frac{1}{\sqrt{-II_{\Omega}}}\left(\mathbf{a}\boldsymbol{\Omega}^2+\boldsymbol{\Omega}^2\mathbf{a}-\frac{2}{3}I_{\mathbf{a}\boldsymbol{\Omega}^2}\mathbf{I}\right) \tag{41}$$

and the tensor basis (40), the following coefficients are achieved

$$\begin{aligned}c_1^{\Omega}=2(&-6V\,I_{\mathbf{a}\boldsymbol{\Omega}^2\mathbf{S}}II_{\Omega^*}^3+4V\,II_{\Omega^*}^2I_{\mathbf{a}\boldsymbol{\Omega}^2\boldsymbol{\Omega}^{*2}\mathbf{S}}+4V\,II_{\Omega^*}^2I_{\mathbf{a}\boldsymbol{\Omega}^2\mathbf{S}\boldsymbol{\Omega}^{*2}}\\&-12V\,II_{\Omega^*}^2IV\,I_{\mathbf{a}\boldsymbol{\Omega}^{*2}}+28V\,I_{\mathbf{a}\boldsymbol{\Omega}^2\boldsymbol{\Omega}^{*2}}IV\,II_{\Omega^*}+I_{\mathbf{a}\boldsymbol{\Omega}^2\mathbf{S}}II_SII_{\Omega^*}^4\\&+2I_{\mathbf{a}\boldsymbol{\Omega}^{*2}}IV\,II_SII_{\Omega^*}^3-6I_{\mathbf{a}\boldsymbol{\Omega}^2\boldsymbol{\Omega}^{*2}}IV\,II_SII_{\Omega^*}^2\\&-4II_{\Omega^*}I_{\mathbf{a}\boldsymbol{\Omega}^2\boldsymbol{\Omega}^{*2}\mathbf{S}}IV^2-4II_{\Omega^*}I_{\mathbf{a}\boldsymbol{\Omega}^2\mathbf{S}\boldsymbol{\Omega}^{*2}}IV^2\\&+8I_{\mathbf{a}\boldsymbol{\Omega}^2\boldsymbol{\Omega}^{*2}}IV^3)/Q_1Q_2\sqrt{-II_{\Omega}}\end{aligned} \tag{42}$$

$$\begin{aligned}c_2^{\Omega}=4(&-8V^2I_{\mathbf{a}\boldsymbol{\Omega}^{*2}}II_{\Omega^*}+24V^2I_{\mathbf{a}\boldsymbol{\Omega}^2\boldsymbol{\Omega}^{*2}}+6V\,II_SI_{\mathbf{a}\boldsymbol{\Omega}^{*2}}II_{\Omega^*}^2\\&-18V\,II_{\Omega^*}II_SI_{\mathbf{a}\boldsymbol{\Omega}^2\boldsymbol{\Omega}^{*2}}+14V\,II_{\Omega^*}IV\,I_{\mathbf{a}\boldsymbol{\Omega}^2\mathbf{S}}-12V\,IV\,I_{\mathbf{a}\boldsymbol{\Omega}^2\mathbf{S}\boldsymbol{\Omega}^{*2}}\\&+8V\,IV^2I_{\mathbf{a}\boldsymbol{\Omega}^{*2}}-12V\,IV\,I_{\mathbf{a}\boldsymbol{\Omega}^2\boldsymbol{\Omega}^{*2}\mathbf{S}}-I_{\mathbf{a}\boldsymbol{\Omega}^{*2}}II_S^2II_{\Omega^*}^3\\&-3II_{\Omega^*}^2IV\,I_{\mathbf{a}\boldsymbol{\Omega}^2\mathbf{S}}II_S+3II_{\Omega^*}^2I_{\mathbf{a}\boldsymbol{\Omega}^2\boldsymbol{\Omega}^{*2}}II_S^2\\&+2II_{\Omega^*}II_SI_{\mathbf{a}\boldsymbol{\Omega}^2\mathbf{S}\boldsymbol{\Omega}^{*2}}IV+2II_{\Omega^*}II_SI_{\mathbf{a}\boldsymbol{\Omega}^2\boldsymbol{\Omega}^{*2}\mathbf{S}}IV\\&-4II_SI_{\mathbf{a}\boldsymbol{\Omega}^2\boldsymbol{\Omega}^{*2}}IV^2+4I_{\mathbf{a}\boldsymbol{\Omega}^2\mathbf{S}}IV^3)/Q_1Q_2\sqrt{-II_{\Omega}}\end{aligned} \tag{43}$$

$$\begin{aligned}c_3^{\Omega}=2(&II_{\Omega^*}I_{\mathbf{a}\boldsymbol{\Omega}^2\mathbf{S}\boldsymbol{\Omega}^{*}}-II_{\Omega^*}I_{\mathbf{a}\boldsymbol{\Omega}^2\boldsymbol{\Omega}^{*}\mathbf{S}}+2I_{\mathbf{a}\boldsymbol{\Omega}^2\boldsymbol{\Omega}^{*}\mathbf{S}\boldsymbol{\Omega}^{*2}}\\&-2I_{\mathbf{a}\boldsymbol{\Omega}^2\boldsymbol{\Omega}^{*2}\mathbf{S}\boldsymbol{\Omega}^{*}})/Q_2\sqrt{-II_{\Omega}}\end{aligned} \tag{44}$$

$$\begin{aligned}c_4^{\Omega}=-4(&-2V\,I_{\mathbf{a}\boldsymbol{\Omega}^2\mathbf{S}}II_{\Omega^*}^2-4V\,IV\,I_{\mathbf{a}\boldsymbol{\Omega}^{*2}}II_{\Omega^*}+12V\,IV\,I_{\mathbf{a}\boldsymbol{\Omega}^2\boldsymbol{\Omega}^{*2}}\\&+II_{\Omega^*}^2II_SI_{\mathbf{a}\boldsymbol{\Omega}^2\boldsymbol{\Omega}^{*2}\mathbf{S}}+II_{\Omega^*}^2II_SI_{\mathbf{a}\boldsymbol{\Omega}^2\mathbf{S}\boldsymbol{\Omega}^{*2}}-2II_{\Omega^*}II_SIV\,I_{\mathbf{a}\boldsymbol{\Omega}^2\boldsymbol{\Omega}^{*2}}\\&+2II_{\Omega^*}IV^2I_{\mathbf{a}\boldsymbol{\Omega}^2\mathbf{S}}+4IV^3I_{\mathbf{a}\boldsymbol{\Omega}^{*2}}-6IV^2I_{\mathbf{a}\boldsymbol{\Omega}^2\boldsymbol{\Omega}^{*2}\mathbf{S}}\\&-6IV^2I_{\mathbf{a}\boldsymbol{\Omega}^2\mathbf{S}\boldsymbol{\Omega}^{*2}})/Q_1Q_2\sqrt{-II_{\Omega}}\end{aligned} \tag{45}$$

$$\begin{aligned}c_5^{\Omega}=4(&-4II_{\Omega^*}V\,I_{\mathbf{a}\boldsymbol{\Omega}^2\boldsymbol{\Omega}^{*}\mathbf{S}}+4II_{\Omega^*}V\,I_{\mathbf{a}\boldsymbol{\Omega}^2\mathbf{S}\boldsymbol{\Omega}^{*}}+6V\,I_{\mathbf{a}\boldsymbol{\Omega}^2\boldsymbol{\Omega}^{*}\mathbf{S}\boldsymbol{\Omega}^{*2}}\\&-6V\,I_{\mathbf{a}\boldsymbol{\Omega}^2\boldsymbol{\Omega}^{*2}\mathbf{S}\boldsymbol{\Omega}^{*}}-II_{\Omega^*}^2II_SI_{\mathbf{a}\boldsymbol{\Omega}^2\mathbf{S}\boldsymbol{\Omega}^{*}}+II_{\Omega^*}^2II_SI_{\mathbf{a}\boldsymbol{\Omega}^2\boldsymbol{\Omega}^{*}\mathbf{S}}\\&-II_SII_{\Omega^*}I_{\mathbf{a}\boldsymbol{\Omega}^2\boldsymbol{\Omega}^{*}\mathbf{S}\boldsymbol{\Omega}^{*2}}+II_SII_{\Omega^*}I_{\mathbf{a}\boldsymbol{\Omega}^2\boldsymbol{\Omega}^{*2}\mathbf{S}\boldsymbol{\Omega}^{*}}-2IV^2I_{\mathbf{a}\boldsymbol{\Omega}^2\boldsymbol{\Omega}^{*}\mathbf{S}}\\&+2IV^2I_{\mathbf{a}\boldsymbol{\Omega}^2\mathbf{S}\boldsymbol{\Omega}^{*}})/Q_1Q_2\sqrt{-II_{\Omega}}\end{aligned} \tag{46}$$

where

$$Q_1 = 2IV^2 + 4II_{\Omega^*}V - II^2_{\Omega^*}II_S Q_2 = -II^2_{\Omega^*}II_S + 4IV^2 + 2II_{\Omega^*}V \quad (47)$$

$I_{\mathbf{X}}$ means the trace of the tensor $\mathbf{X}$.

Applying the same procedure to

$$\mathbf{N}_S = \frac{1}{\sqrt{II_S}}\left(\mathbf{aS}^2 + \mathbf{S}^2\mathbf{a} - \frac{2}{3}I_{\mathbf{aS}^2}\mathbf{I}\right) \quad (48)$$

gives the corresponding representation coefficients

$$\begin{aligned} c_1^S = &-(18V\,II_S I_{\mathbf{aS}} II^3_{\Omega^*} + 72V\,II^2_{\Omega^*}IV\,I_{\mathbf{aS}^2} - 24V\,II^2_{\Omega^*}I_{\mathbf{aS}^2\mathbf{\Omega}^{*2}\mathbf{S}} \\ &- 12V\,II^2_{\Omega^*}II_S I_{\mathbf{aS\Omega}^{*2}} - 8V\,II^2_{\Omega^*}III_S I_{\mathbf{a\Omega}^{*2}} \\ &- 168V\,I_{\mathbf{aS}^2\mathbf{\Omega}^{*2}}IV\,II_{\Omega^*} - 3II^2_S I_{\mathbf{aS}} II^4_{\Omega^*} - 12I_{\mathbf{aS}^2}IV\,II_S II^3_{\Omega^*} \\ &+ 36I_{\mathbf{aS}^2\mathbf{\Omega}^{*2}}IV\,II_S II^2_{\Omega^*} + 8II_{\Omega^*}III_S I_{\mathbf{a\Omega}^{*2}}IV^2 \\ &+ 12II_{\Omega^*}II_S I_{\mathbf{aS\Omega}^{*2}}IV^2 + 24II_{\Omega^*}I_{\mathbf{aS}^2\mathbf{\Omega}^{*2}\mathbf{S}}IV^2 \\ &- 48I_{\mathbf{aS}^2\mathbf{\Omega}^{*2}}IV^3)/3Q_1Q_2\sqrt{II_S} \end{aligned} \quad (49)$$

$$\begin{aligned} c_2^S = &\,2(-48V^2II_{\Omega^*}I_{\mathbf{aS}^2} + 144V^2I_{\mathbf{aS}^2\mathbf{\Omega}^{*2}} + 36V\,II_S I_{\mathbf{aS}^2}II^2_{\Omega^*} \\ &- 108V\,II_{\Omega^*}II_S I_{\mathbf{aS}^2\mathbf{\Omega}^{*2}} + 42V\,II_{\Omega^*}IV\,II_S I_{\mathbf{aS}} + 48V\,IV^2I_{\mathbf{aS}^2} \\ &- 36V\,IV\,II_S I_{\mathbf{aS\Omega}^{*2}} - 72V\,IV\,I_{\mathbf{aS}^2\mathbf{\Omega}^{*2}\mathbf{S}} - 24V\,IV\,III_S I_{\mathbf{a\Omega}^{*2}} \\ &- 6I_{\mathbf{aS}^2}II^2_S II^3_{\Omega^*} - 9II^2_{\Omega^*}IV\,II^2_S I_{\mathbf{aS}} + 18II^2_{\Omega^*}I_{\mathbf{aS}^2\mathbf{\Omega}^{*2}}II^2_S \\ &+ 12II_{\Omega^*}II_S I_{\mathbf{aS}^2\mathbf{\Omega}^{*2}\mathbf{S}}IV + 6II_{\Omega^*}II^2_S I_{\mathbf{aS\Omega}^{*2}}IV \\ &+ 4II_{\Omega^*}II_S III_S I_{\mathbf{a\Omega}^{*2}}IV - 24II_S I_{\mathbf{aS}^2\mathbf{\Omega}^{*2}}IV^2 \\ &+ 12II_S I_{\mathbf{aS}}IV^3)/3Q_1Q_2\sqrt{II_S} \end{aligned} \quad (50)$$

$$\begin{aligned} c_3^S = &\,(II_{\Omega^*}II_S I_{\mathbf{aS\Omega}^*} - 2II_{\Omega^*}I_{\mathbf{aS}^2\mathbf{\Omega}^*\mathbf{S}} + 4I_{\mathbf{aS}^2\Omega^*\mathbf{S}\Omega^{*2}} \\ &- 4I_{\mathbf{aS}^2\mathbf{\Omega}^{*2}\mathbf{S\Omega}^*})/Q_2\sqrt{II_S} \end{aligned} \quad (51)$$

$$\begin{aligned} c_4^S = &\,2(6V\,II_S I_{\mathbf{aS}} II^2_{\Omega^*} + 24V\,IV\,I_{\mathbf{aS}^2}II_{\Omega^*} - 72V\,I_{\mathbf{aS}^2\mathbf{\Omega}^{*2}}IV \\ &- 3II^2_{\Omega^*}II^2_S I_{\mathbf{aS\Omega}^{*2}} - 6II^2_{\Omega^*}II_S I_{\mathbf{aS}^2\mathbf{\Omega}^{*2}\mathbf{S}} - 2II^2_{\Omega^*}II_S III_S I_{\mathbf{a\Omega}^{*2}} \\ &- 6II_{\Omega^*}II_S I_{\mathbf{aS}}IV^2 + 12II_{\Omega^*}I_{\mathbf{aS}^2\mathbf{\Omega}^{*2}}IV\,II_S + 36I_{\mathbf{aS}^2\mathbf{\Omega}^{*2}\mathbf{S}}IV^2 \\ &+ 18II_S I_{\mathbf{aS\Omega}^{*2}}IV^2 - 24I_{\mathbf{aS}^2}IV^3 \\ &+ 12III_S I_{\mathbf{a\Omega}^{*2}}IV^2)/3Q_1Q_2\sqrt{II_S} \end{aligned} \quad (52)$$

$$\begin{aligned} c_5^S = &\,2(4II_S I_{\mathbf{aS\Omega}^*}II_{\Omega^*}V - 8I_{\mathbf{aS}^2\mathbf{\Omega}^*\mathbf{S}}II_{\Omega^*}V + 12V\,I_{\mathbf{aS}^2\Omega^*\mathbf{S}\Omega^{*2}} \\ &- 12V\,I_{\mathbf{aS}^2\mathbf{\Omega}^{*2}\mathbf{S\Omega}^*} + 2I_{\mathbf{aS}^2\mathbf{\Omega}^*\mathbf{S}}II^2_{\Omega^*}II_S - II^2_S I_{\mathbf{aS\Omega}^*}II^2_{\Omega^*} \\ &+ 2II_{\Omega^*}II_S I_{\mathbf{aS}^2\mathbf{\Omega}^{*2}\mathbf{S\Omega}^*} - 2II_{\Omega^*}II_S I_{\mathbf{aS}^2\Omega^*\mathbf{S}\Omega^{*2}} \\ &+ 2II_S I_{\mathbf{aS\Omega}^*}IV^2 - 4I_{\mathbf{aS}^2\mathbf{\Omega}^*\mathbf{S}}IV^2)/Q_1Q_2\sqrt{II_S} \end{aligned} \quad (53)$$

In order to derive the EARSM using projected $\mathbf{N}^{\Omega}$ and $\mathbf{N}^{S}$, as given above, the invariants I first have to be calculated by inserting $\mathbf{a}$ expressed in (40). Since the different c_i^S and c_i^{Ω} coefficients are linear in $\mathbf{a}$, the corresponding ARSM system of equations will remain linear (except for the $I_{\mathbf{aS}}$ nonlinearity) and may be solved. However, the algebra is significantly more complex than in the original EARSM. The alternative is to use the projection approach on the ARSM equation directly. This would of course lead to the same result.

Appendix B. EARSM platform equations

For the homogeneous rotating shear flow computations, the two equation platform used consists of the standard equations for the turbulence kinetic energy, K, and its dissipation, ε,

$$\frac{\mathrm{d}K}{\mathrm{d}t} = \mathscr{P} - \varepsilon \quad (54)$$

$$\frac{\mathrm{d}\varepsilon}{\mathrm{d}t} = \frac{\varepsilon}{K}(C_{\varepsilon 1}\mathscr{P} - C_{\varepsilon 2}\varepsilon) \quad (55)$$

where the diffusion has been neglected since the flow is homogeneous. The production of K is given by

$$\mathscr{P} = -\varepsilon a_{ij}S_{ji} \quad (56)$$

in which a_{ij} is the Reynolds stress anisotropy and S_{ij} is defined as in (2). The model parameters are $C_{\varepsilon 1} = 1.56$ and $C_{\varepsilon 2} = 1.83$, which makes the K–ε platform equivalent to the K–ω platform for homogeneous flows.

For the computations of rotating channel and pipe flow, the standard K–ω platform was used. The governing equations can be written

$$\frac{\partial K}{\partial t} = \mathscr{P} - \beta^*\omega K + \frac{\partial}{\partial x_i}\left(\left(\nu + c_s\frac{K}{\varepsilon}\overline{u_iu_j}\right)\frac{\partial K}{\partial x_j}\right) \quad (57)$$

$$\frac{\partial \omega}{\partial t} = \alpha\frac{\omega}{K}\mathscr{P} - \beta\omega^2 + \frac{\partial}{\partial x_i}\left(\left(\nu + c_{se}\frac{K}{\varepsilon}\overline{u_iu_j}\right)\frac{\partial \omega}{\partial x_j}\right) \quad (58)$$

$c_s = 0.1$ and $c_{se} = 0.09$ are the diffusion model parameters. The parameter values were achieved by considering the log-layer of channel flow and to approximately match the corresponding eddy-viscosity diffusion models in the Wilcox (1988) K–ω model.

$\mathscr{P}$ is given by (56) and the dissipation rate of the turbulence kinetic energy is related to K and ω as

$$\varepsilon \equiv \beta^*\omega K \quad (59)$$

The only near wall treatment used is a lower limit of the turbulence timescale

$$\tau = \max\left(\frac{K}{\varepsilon}, C_\tau\sqrt{\frac{\nu}{\varepsilon}}\right) \quad (60)$$

This was proposed by Durbin (1993) and is just the usual timescale with a lower bound given by the Kolmogorov scale. The values of the model parameters are

$$\alpha = \frac{5}{9}, \quad \beta = \frac{3}{40}, \quad \beta^* = 0.09, \quad C_\tau = 6.0 \quad (61)$$

References

Alvelius, K., 1999. Studies of turbulence and its modelling through large eddy- and direct numerical simulation, Ph.D. Thesis, Department of mechanics, KTH, Stockholm, Sweden.

Bardina, J., Ferziger, J.H., Reynolds, W.C., 1983. Improved turbulence models based on large-eddy simulation of homogeneous, incompressible turbulent flows, Stanford University Technical Report, TF-19.

Daly, B.J., Harlow, F.H., 1970. Transport equations in turbulence. Phys. Fluids 13, 2634–2649.

Durbin, P.A., 1993. Application of near-wall turbulence model to boundary layers and heat transfer. Int. J. Heat Fluid Flow 13, 316–323.

Gatski, T.B., Jongen, T., 2000. Nonlinear eddy viscosity and algebraic stress models for solving complex turbulent flows. Progr. Aerospace Sci. 38, 655–682.

Gatski, T., Wallin, S., 2004. Extending the weak-equilibrium condition for algebraic Reynolds stress models to rotating and curved flows. J. Fluid Mech. 518, 147–155.

Girimaji, S.S., 1997. A Galilean invariant explicit algebraic Reynolds stress model for turbulent curved flows. Phys. Fluids 9, 1067–1077.

Imao, S., Itoh, M., Harada, T., 1996. Turbulent characteristics of the flow in an axially rotating pipe. Int. J. Heat Fluid Flow 17, 444–451.

Johansson, A.V., 1995. The hierarchy of one-point closures and the modelling of rotational effects. In: Benzi, R. (Ed.), Advances in Turbulence V, Proc. the Fifth European Turbulence Conference, Siena, July 1994. Kluwer, pp. 251–255.

Johansson, A.V., Hallbäck, M., 1994. Modelling of rapid pressure–strain in Reynolds-stress closures. J. Fluid Mech. 269, 143–168.

Jongen, T., Gatski, T.B., 1998. General explicit algebraic stress relations and best approximation for three-dimensional flows. Int. J. Eng. Sci. 36, 739–763.

Kassinos, S.C., Reynolds, W.C., Rogers, M.M., 2001. One-point turbulence structure tensors. J. Fluid Mech. 428, 213–248.

Leuchter, O., Cambon, C., 1996. Spectral analysis of rotation effects on axisymmetrically strained turbulence with an improved EDQNM model. In: Proc. the Sixth European Turbulence, Lausanne, 2–5 July 1996.

Mansour, N.N., Shih, T.H., Reynolds, W.C., 1991. The effects of rotation on initially anisotropic homogeneous flows. Phys. Fluids 3, 2421–2425.

Poroseva, S.V., Kassinos, S.C., Langer, C.A., Reynolds, W.C., 2002. Structure-based turbulence model: application to a rotating pipe flow. Phys. Fluids 14, 1523–1532.

Rodi, W., 1976. A new algebraic relation for calculating the Reynolds stresses. Z. Angew. Math. Mech. 56, 219–221.

Sjögren, T., 1997. Development and validation of turbulence models through experiment and computation. Ph.D. Thesis, Department of Mechanics, KTH, Stockholm, Sweden.

Sjögren, T., Johansson, A.V., 2000. Development and calibration of algebraic nonlinear models for terms in the Reynolds stress transport equations. Phys. Fluids 12, 1554–1572.

Speziale, C.G., Sarkar, S., Gatski, T.B., 1991. Modelling the pressure–strain correlation of turbulence: an invariant dynamical systems approach. J. Fluid Mech. 227, 245–272.

Taulbee, D.B., 1992. An improved algebraic Reynolds stress model and corresponding nonlinear stress model. Phys. Fluids A 4, 2555–2561.

Taulbee, D.B., Sonnenmeier, J.R., Wall, K.M., 1994. Stress relation for three-dimensional turbulent flows. Phys. Fluids 6, 1399–1401.

Wallin, S., Johansson, A.V., 2000. An explicit algebraic Reynolds stress model for incompressible and compressible turbulent flows. J. Fluid Mech. 403, 89–132.

Wallin, S., Johansson, A.V., 2002. Modelling streamline curvature effects in explicit algebraic Reynolds stress turbulence models. Int. J. Heat Fluid Flow 23, 721–730.

Wilcox, D.C., 1988. Reassessment of the scale-determining equation for advanced turbulence models. AIAA J. 26, 1299–1310.